

# Force-dependent Piezo1 recruitment to focal adhesions regulates adhesion maturation and turnover specifically in non-transformed cells

Mingxi Yao<sup>1</sup>, Ajay Tijore<sup>1</sup>, Charles D Cox<sup>2</sup>, Anushya Hariharan<sup>1</sup>, Guy Tran Van Nhieu<sup>3</sup>, Boris Martinac<sup>2</sup>, Michael Sheetz<sup>\*1,4,5</sup>

1. Mechanobiology Institute, National University of Singapore
2. Victor Chang Cardiac Research Institute
3. Collège de France
4. Dept of Biological Sciences, National University of Singapore
5. Molecular MechanoMedicine Program, Dept. of Biochemistry and Molecular Biology, UTMB, Galveston, TX 77555

\*Correspondence: [misheetz@utmb.edu](mailto:misheetz@utmb.edu)

## *Abstract:*

Piezo1 is a mechanosensitive Ca<sup>2+</sup>-permeable channel that has been implicated in a number of mechanosensing processes. It is diffusive on plasma membranes and activated by local membrane tension changes yet recent data suggest that Piezo1 activity is tightly coupled to the integrin-mediated actin cytoskeleton through a poorly understood mechanism. In our studies, we found that Piezo1 stably localizes to RGD matrix adhesions in normal but not in transformed cells. Piezo1 binding requires contractility and triggers local Ca<sup>2+</sup> entry during adhesion formation and turnover. In transformed cells, Piezo1 level does not affect adhesion morphology; and there is no detectable Ca<sup>2+</sup> influx around adhesions. Based upon these findings, we suggest that Piezo1 is a novel component of integrin-based adhesions in non-transformed cells and contributes to the distinct mechanosensing and Ca<sup>2+</sup> signaling in normal vs transformed cells. Concentration of Piezo1 at adhesions is a key factor underlying Piezo1's physiological functions.

## Introduction

Since the discovery of Piezo1 as a mechanosensitive ion channel responsible for mechanically activated currents in 2010, its roles in important biological processes have gained increasing attention<sup>1-4</sup>. Of the two members of the *piezo* family (Piezo1 and Piezo2), Piezo1 is widely expressed in somatic cell types and is a crucial mechanosensor in physiological processes such as stem cell lineage determination, blood pressure regulation, activation of innate immunity and vascular development<sup>1,5-7</sup>. Piezo1 knock-out is embryonically lethal in mice during mid-gestation stage due to vascular defects<sup>5</sup>. Many gain- and loss-of-function mutants of Piezo1 are linked to hereditary diseases such as hereditary anemia (xerocytosis) and generalized lymphatic dysplasia<sup>8,9</sup>.

Piezo1 gene encodes a large protein of more than 2500 amino acids, with 38 transmembrane helices<sup>10</sup>. In the plasma membrane, Piezo1 forms a propeller shaped homo-trimer structure that consists of a central ion-conducting pore and three helical-bundle peripheral blades linked to the pore through long lever-like intracellular beams<sup>10</sup>. Upon mechanical stimulation, Piezo1 undergoes a short activation phase that allows Ca<sup>2+</sup> entry, which is followed by an inactivation phase that makes it insensitive to further stimulation<sup>11</sup>. Biophysical studies have shown that membrane bilayer tension changes can directly activate Piezo1 ion channels and the regulation of Piezo1's function has been attributed to the regulation of localized lipid bilayer tension changes<sup>12,13</sup>. This is supported by biophysical studies that Piezo1 is sensitive to specific lipid types<sup>14</sup> and the observations that Piezo1 is diffusively localized in plasma membranes of many cell lines with very few interaction partners identified<sup>4,13,15,16</sup>. However, an open question in the regulation of Piezo1 is the intimate involvement of the integrin-linked actin cytoskeleton in Piezo1's functions<sup>17</sup>. Before the discovery of Piezo1 as a mechanosensitive ion channel, Piezo1 was shown to be involved in integrin activation<sup>18</sup>. The activation of Piezo1 is regulated by the actin cytoskeleton as well<sup>17</sup>. When N2A cells are mechanically agitated with micron-sized, collagen IV or Matrigel coated beads, the tension threshold required to trigger Piezo-dependent Ca<sup>2+</sup> entry is significantly reduced<sup>19</sup>. In addition, integrin signaling pathways are critical for

proper function of Piezo1 in the context of endothelial cell responses to flow<sup>20</sup>. These data indicate a tight coupling between Piezo1 signaling and integrin based mechanosensing functions of cells.

Local Ca<sup>2+</sup> signaling is an integral component of physiological activities such as adhesion maturation, cell survival, proliferation, migration and differentiation<sup>21–23</sup>. Although cancer cells share many activities with normal cells, there is evidence of increased calpain activity and Ca<sup>2+</sup> sensitivity in cancer cells<sup>24</sup>. Exploiting the differences between Ca<sup>2+</sup> signaling pathways of normal and malignant transformed cells may provide potentially viable strategies to specifically target cancer cells. We and others have shown previously that a fundamental difference between the transformed and normal phenotype is the response to cyclic stretch, which promotes the spreading and proliferation of normal cells but leads to Ca<sup>2+</sup> accumulation and apoptosis for transformed cells<sup>2,25,26</sup>. In the screening for the Ca<sup>2+</sup> channels responsible for cyclic-stretch dependent Ca<sup>2+</sup> entry in transformed cells, we determined that the mechanosensitive ion channel Piezo1 was essential<sup>26</sup>. Depletion of Piezo1 in transformed cell lines such as MDA-MB-231 and HEK 293T inhibited cyclic-stretch dependent apoptosis. Interestingly, in normal cells such as human foreskin fibroblast with comparable Piezo1 expression levels, cyclic stretching did not induce Ca<sup>2+</sup> build-up and apoptosis<sup>26</sup>. These results imply an important regulatory role for Piezo1 in Ca<sup>2+</sup> signaling of normal vs transformed cells.

Here, we show that in many normal cell lines including fibroblastic, epithelial and endothelial lines, Piezo1 is enriched at focal adhesions in a force dependent manner. In contrast, in transformed cells that lack rigidity sensing, Piezo1 is diffusely distributed and recovers completely in FRAP experiments. For the normal cells, focal adhesion formation, turnover and force generation require Piezo1 that acts through calpain-dependent pathways. These studies suggest that Piezo1 functions as a major sensor of mechanical cues in mechanosensing processes that function distinctively in normal versus transformed cells and its activity is regulated by both membrane tension and membrane-associated adhesion complexes that include cytoskeletal connections.

## Results

### *Piezo1 stably localizes to mature adhesions in HFF cells*

To investigate the role of Piezo1 in adhesion formation, we followed the distribution and dynamics of Piezo1 localization during cell spreading. Transiently expressed Piezo1 tagged with GFP or mRuby3 and paxillin-BFP were followed during the cell spreading in primary human foreskin fibroblast cells (HFF) (Figure 1A top panel, supplementary movie 1). The Piezo1 fluorescent tags were inserted in the long intracellular loop region at site 1591 to minimize the disruption of the channel opening properties of Piezo1 by the fluorescent tag<sup>13</sup>. In the initial phase of spreading, Piezo1 did not colocalize with cell adhesions marked by paxillin and appeared concentrated in the central part of the cell. After 30-60 minutes when the cell developed mature adhesions, Piezo1 dispersed to the entire spread area of the cell and was significantly enriched in maturing adhesions.

Piezo1 localization to adhesions increased over time until the cell began to polarize. Upon cell polarization, Piezo1 preferentially localized to the retracting edges (Figure 1B, upper panel). After spreading overnight, HFF cells reached a dynamic steady state and Piezo1 was enriched at mature focal adhesions (Figure 1B, middle panel). In most cells, Piezo1 was recruited to a sub population of all the focal adhesions, mostly around cell periphery and at the ends of stress fibers inside of the cells. Piezo1 was often recruited to a portion of a single focal adhesion as well (Figure 1B lower panel, marked by arrow), implying a very local regulation of Piezo1 recruitment. The localization of endogenous Piezo1 to adhesions in HFF cells was also observed by Piezo1 immunostaining of fixed HFF cells (Figure S1) using a knockdown validated antibody<sup>2</sup>. Thus, Piezo1 complexed with mature and retracting adhesions in polarized cells.

Since Piezo1 was previously reported to be diffusive in plasma membranes, we checked the lifetime of Piezo1 in the focal adhesions of HFF cells by Fluorescence Recovery After Photobleaching (FRAP assay). Surprisingly, as shown in Figure 1C, Piezo1 was stable at the adhesions after recruitment, with turnover time of around 120s, considerably lower compared to typical focal adhesion proteins such as paxillin ~25s and

even slightly less than integrins such as integrin  $\beta 3 \sim 90s$  (Figure 1D). In addition, the mobile fraction of Piezo1 was considerably less than the mobile fraction of paxillin and even integrin  $\beta 3$  (Figure 1D). These data indicated that Piezo1 formed stable interactions with certain focal adhesion components in HFF cells.

### *Piezo1 recruitment to adhesions requires myosin II contractility*

Since focal adhesion maturation was linked to sustained traction forces and correlated with Piezo1 recruitment during spreading, we hypothesized that Piezo1-adhesion interactions were force dependent. Treatment of Piezo1-GFP expressing HFF cells with 30  $\mu M$  of Y23762 to inhibit actomyosin contraction, caused rapid loss of Piezo1 from adhesion sites and was followed by the disassembly of focal adhesions as measured by paxillin (Figure 2A, top panel, supplementary movie2). Similar results were observed with 50  $\mu M$  blebbistatin treatment (Figure S2A). When Y-23762 was washed out, Piezo1 returned rapidly to newly formed adhesions (Figure 2A, top panel). Since Piezo1 recruitment on recovery was much more rapid than the initial recruitment to adhesions during cell spreading (minutes versus hours), we postulated that components remaining at adhesions in the absence of force catalyzed the rapid recovery of adhesion proteins with the development of contractile forces to enable Piezo1 binding. Further, when the contractility of the cell was enhanced by co-expressing constitutively active version of RhoA along with Piezo1 in HFF cells or in FAK  $-/-$  MEF cells that have elevated RhoA activity<sup>27</sup>, the enrichment of Piezo1 to adhesions was strongly promoted (Figure 2A, bottom panel).

To check whether the reduction of traction forces alone could disrupt Piezo1's adhesion recruitment without disruption of adhesion proteins such as talin and integrins, we tested the relationship between Piezo1 localization and myosin II contractility in intact adhesions. Previous reports showed that inhibition of tyrosine phosphatase PTP-PEST, as well as the expression of virulence bacterial protein IpaA, inhibited adhesion disassembly upon treatment of Y-compound<sup>28,29</sup>. In cells expressing GFP-labelled IpaA peptide, addition of 30  $\mu M$  Y-compound caused cells to lose contractility while retaining adhesion structures (Figure 2B, Supplemental movie 3). In this case, Piezo1-mRuby3 diffused out from adhesions within 10 min after Y compound treatment while the integrin  $\beta 3$ -BFP remained intact. A similar effect was observed when 2.5  $\mu M$

of PTP-PEST inhibitor was added in combination with 30  $\mu$ M Y-compound (Figure S2B). Thus, the localization of Piezo1 to focal adhesions depended on continued contraction forces, and was independent of paxillin localization to adhesions possibly through the stretching of adhesion proteins.

To further establish the role of myosin II-based contractility in Piezo1 recruitment, we checked the distribution of Piezo1 in cells that had low traction forces such as COS-7 cells which lacked myosin IIA expression<sup>30</sup>. In COS-7 cells transiently expressing Piezo1-GFP and paxillin-mapple, Piezo1 was diffusive in the membrane with no apparent localization to adhesions (Figure 2C, top panel) and the cell adopted a highly-spread disc morphology. When contractility was restored in COS-7 cells by overexpressing myosin IIA, cells became polarized with myosin IIA forming stress-fiber-like cables (Figure 2C, bottom panel) and Piezo1 was recruited to the adhesions at the ends of the myosin cables. This further reinforced the hypothesis that Piezo1 recruitment to adhesions required continued force on the adhesion complex.

### *Piezo1 localization to adhesions during spreading depends on matrix.*

We then checked if different matrices that engaged different integrins regulated the recruitment of Piezo1. HFF cells transiently transfected with Piezo1-mruby3 were seeded overnight on a variety of ECM substrates including fibronectin, vitronectin, collagen I and laminin that preferentially activated different sets of integrins and the area fraction of the focal adhesions with Piezo1 recruitment was checked<sup>31</sup>. Interestingly, we found enhanced Piezo1 recruitment to adhesions on fibronectin and vitronectin surfaces but reduced Piezo1 recruitment on laminin and collagen I coated surfaces. (Figure 3 A-B). Changes in traction forces on these ECM surfaces were insufficient to account for the differential Piezo1 recruitment, since co-expression of constitutively active RhoA led to higher Piezo1 recruitment on vitronectin and fibronectin surfaces but not on laminin surfaces (Figure 3A provides a representative example).

We examined if Piezo1's recruitment to adhesions might be linked to specific types of integrins. When HFF cells spreading on fibronectin surfaces were stained for  $\alpha$ V $\beta$ 3 (LM609 antibody) and activated  $\beta$ 1 (9EG7 antibody), both integrins were co-localized with Piezo1 at focal adhesions in most cases (Figure 3 A). On laminin surfaces where Piezo1 was not localized to adhesions, antibody staining indicated low  $\alpha$ V $\beta$ 3 and

strong activation of  $\beta 1$  at focal adhesions consistent with previous reports (Figure 3A). We thus checked the possibility that Piezo1 localization to adhesions was promoted by RGD-based integrins such as  $\alpha V\beta 3$ . When HFF cells were pretreated with RGD-blocker cilengitide and seeded on collagen I surfaces, significantly weaker Piezo1 recruitment to paxillin adhesions was observed<sup>32</sup> (Figure 3C). These data supported a role of RGD-based  $\alpha V\beta 3$  adhesions in Piezo1 recruitment. Similar results were observed with immunostaining of endogenous Piezo1 in wildtype HFF cells seeded on various ECM substrates (Figure S3).

### *Piezo1 recruitment triggers (calpain dependent) adhesion turnover in an integrin specific manner*

Since Piezo1 recruitment to adhesions was linked to RGD-based integrins during cell spreading, we analyzed the colocalization of Piezo1 with  $\beta 3$  adhesions during cycles of adhesion assembly and disassembly. Interestingly, the recruitment of Piezo1 to  $\beta 3$ -enriched adhesions correlated with the disassembly and turnover of the  $\beta 3$  adhesions. Figure 4A shows the timelapse views of two examples of such turnover events on fibronectin surfaces, one during spreading where the cell was protruding and the other in migrating cells where the adhesion was retracting. In both cases, integrin  $\beta 3$ -based adhesions formed without apparent Piezo1 co-localization. Over time, Piezo1 was recruited to the adhesions from the periphery of the adhesions and gradually occupied the whole adhesion. Piezo 1 recruitment appeared to initiate a decrease in integrin  $\beta 3$  fluorescence intensity within minutes (Figure 4A and supplementary movie 4-5). After integrin  $\beta 3$  reached background levels, the Piezo1 fluorescence often persisted in adhesions for a few minutes before dissociation (Figure 4A, Left panel, arrows; Figure S4A gives a detailed profile), indicating that some adhesion components remained that supported Piezo1 localization.

Interestingly, the anticorrelated behavior was not observed between Piezo1 and  $\beta 1$  integrins. Piezo1 recruitment at integrin  $\beta 1$  enriched adhesions was more stable, and they often co-localized for tens of minutes (Figure 4B). In an interesting example (Figure S4B), Piezo1 recruitment correlated with the rapid dissociation of  $\beta 3$  integrins and enrichment of  $\beta 1$  integrins. Piezo1 recruitment persisted in adhesions even

after dissociation of  $\beta 1$  integrins (Fig. S4B, arrows). These observations indicated that Piezo1 recruitment was associated with adhesion turnover that was regulated locally in an integrin  $\beta 3$  dependent manner.

Considering Piezo1's function as a mechanosensitive  $\text{Ca}^{2+}$  channel, adhesion turnover was likely caused by the calpain-dependent cleavage pathway. Indeed, when we blocked calpain activity using the inhibitor ALLN, adhesion turnover from the back of the sliding adhesions was inhibited, causing significant elongation of the adhesions (Figure 4C, left panel). However, the translocation speed of adhesions was not altered (Supplementary Movie 4, 5). Piezo1 remained in adhesions following ALLN addition in HFF (Figure 4C). Thus, normal dynamics of  $\beta 3$  adhesions depended upon calpain activity that was likely regulated by local  $\text{Ca}^{2+}$  entry induced by Piezo1's channel activity.

Based upon these findings we suggest that Piezo1 recruitment was upstream of calpain in regulating adhesion turnover. In earlier studies of fibronectin spreading, integrin  $\beta 3$  adhesions formed initially, and then the adhesions switched to integrin  $\beta 1$ . The greater stability of  $\beta 1$ -containing adhesions after Piezo1 recruitment could potentially provide a mechanistic explanation for such switching events<sup>33</sup>.

### *Piezo1 localization to adhesions is lost in transformed cells*

To check whether Piezo1 localization to adhesions was also present in other cell types than HFF, we expressed Piezo1 in several cell lines including fibroblasts (Mouse embryonic fibroblasts), endothelial cells (HUVEC) and several transformed cell lines (MDA-MB-231, HEK293T, A2058) (Figure 5A). Interestingly, in the non-transformed cell lines such as fibroblasts and endothelial cells, Piezo1 localized to adhesions on fibronectin surfaces. However, in the transformed cell lines tested, Piezo1 was diffusive in the plasma membranes and not associated with adhesions. In the MDA-MB-231 breast cancer line, FRAP measurements of Piezo1 diffusion showed that Piezo1 had a significantly higher mobile fraction than in HFF cells (Figure 5B). Similar observations were found with immunostaining of native Piezo1 in HFF and MDA-MB-231 cells (Figure S5A). The difference in Piezo1 immobilization was not due to different levels of Piezo1 expression, since Western blots showed similar levels of Piezo1 in these cell lines (Figure S5B).



Because MDA-MB-231 cells had low levels of integrin  $\beta 3$  expression<sup>34</sup>, it was possible that Piezo1 localization in transformed cells was dependent upon the expression levels of integrin subtypes. To test this possibility we analyzed the melanoma A2058 cells where integrin  $\beta 3$  signaling was essential for their survival and metastasis<sup>35</sup>. As shown in Figure 5A, Piezo1 did not localize to paxillin adhesions in those cells. In addition, in the transformed Chinese Hamster Ovary cell line (CHOB2) that did not express  $\beta 1$  or  $\beta 3$  integrins, the Piezo1 distribution was checked after expression of either  $\alpha 5\beta 1$  or  $\alpha V\beta 3$ . Interestingly, despite the distinct morphology of  $\alpha 5\beta 1$  and  $\alpha V\beta 3$  adhesions in transfected CHOB2 cells, Piezo1 was diffusive in both cell lines (Figure 5C). These results supported the notion that localization of Piezo1 to adhesions was a feature of normal but not transformed cells.

Our previous studies showed that TPM 2.1 levels were low in many transformed cells<sup>25</sup>. Knocking down TPM 2.1 in HFF cells caused the cells to become transformed with smaller adhesions and the cells were not able to differentiate between soft and rigid surfaces, while restoring TPM 2.1 expression in MDA-MB-231 cells leads to escape transform state, form bigger adhesions and fail to survive on soft agar<sup>25</sup>. Based on this, we checked if toggling between non-transformed and transformed state in HFF and MDA-MB-231 cells altered the localization of Piezo1 in these cell lines. When we knocked down TPM 2.1 in HFF cells, the recruitment of Piezo1 to adhesions was significantly weakened compared with control cells or control siRNA-treated cells (Figure S6 A, B). Consistently, when we transiently expressed TPM 2.1-YFP in MDA-MB-231 cells, a significant fraction of cells formed stress fibers and Piezo1 was recruited to adhesions at the end of stress fibers. Like non-transformed HFF cells, expression of constitutively active RhoA enhanced the formation of stress fibers and Piezo1 adhesion recruitment (Figure S6C). These data indicated that there was a correlation between cell transformation and Piezo1 adhesion localization and we recently showed that transformation resulted from the loss of rigidity sensing that was observed in all tumor cells<sup>25</sup>. Thus, the change in cell state between normal and transformed cells resulted in adhesions that did not support Piezo1 binding.

## *Piezo1 recruitment regulates the adhesion morphology and induces local $Ca^{2+}$ influx at adhesions in normal but not in transformed cells*

To determine if Piezo1 was functionally involved in adhesion formation in non-transformed and transformed cells, we knocked down Piezo1 in HFF cells and MDA-MB-231 cells and checked if their spreading was altered. As shown in Figure 6A, Piezo1 knock-down HFF cells spread to smaller areas and had smaller adhesions, while in the transformed MDA-MB-231 cells, knock down of Piezo1 caused significant reduction of cell spreading area but had no effect on adhesion morphology (Figure 6 A-C). This indicated that Piezo1 was important for adhesion maturation in normal cells but did not affect adhesion formation of transformed cells. Previous studies documented that transformed cell lines including cancer cells generally had smaller and less mature adhesions compared with non-transformed cells. This was despite the fact that the majority of adhesion components were present at similar levels in both normal and transformed cells. Thus, Piezo1 recruitment to adhesions in normal cell appeared involved in important steps in the adhesion maturation process.

Recent studies by Ellefsen et. al, showed that Piezo1-dependent calcium spikes were localized to the cell periphery near focal adhesions<sup>15</sup>. This implied that calcium spikes occurred near where high traction forces were generated. In transformed cancer cells, our recent studies showed that transformed cell lines such as MDA-MB-231 and HEK 293T, would undergo calcium-dependent apoptosis upon stretch. The stretch-induced apoptosis of transformed cells was abolished in Piezo1 knock-out cells<sup>26</sup>. This indicated that the calcium uptake by cancer cells was abnormal and so we checked whether calcium spiking was altered with transformation by loading cells with the cell-permeable calcium indicator Cal-520 before measuring calcium levels on fibronectin surfaces. A pulsed laser TIRF system was used to minimize the photo-toxicity of the calcium dye. Similar to the observations by Ellefsen et al, in normal HFF cells, calcium entry localized to areas of high contractility such as the cell edge and surrounding adhesions. Although the transformed MDA-MB-231 cells generated higher local traction forces<sup>25</sup> and were killed by calcium-dependent apoptosis after stretch<sup>26</sup>, they had very few calcium spikes on fibronectin surfaces (Figure 6D-E). Thus, the formation of

mature focal adhesions in the normal cells correlated with calcium spiking but spiking was lost in transformed cells that had smaller adhesions.

## *Discussion*

In this study, we show that Piezo1 localizes to focal adhesions in normal cells but not in transformed cells. Normal fibroblasts, epithelial and endothelial cells form focal adhesions on fibronectin where Piezo1 concentrates in a force-dependent process. However, on laminin and collagen surfaces there is little or no Piezo1 at focal adhesions, due to the selectivity of Piezo1 for RGD-binding integrins. The lifetime of Piezo1 in the adhesions is similar to that of integrins and longer than typical adhesion proteins, which implies that it may complex stably with adhesion bound proteins. Piezo1 localization to adhesions depends on sustained contraction forces and when contraction is inhibited, it leaves adhesions before the dissociation of stable adhesion components such as integrin and talin. This localization is lost in transformed cells, including virus-transformed somatic cells as well as tumor cell lines from different tissues. When somatic cells are induced to become transformed such as in the case of TPM 2.1 knock down, the recruitment of Piezo1 to adhesions is dramatically reduced similar to the transformed cancer lines tested.  $Ca^{2+}$  spiking is found in normal cells at or near matrix adhesions, but spiking is lost upon transformation. In contrast, the transformed cells are sensitive to Piezo1-dependent  $Ca^{2+}$  entry upon stretch that induces apoptosis<sup>26</sup>. These findings indicate that Piezo1 has a number of complex interactions, which depend upon contractility, the transformed state, as well as matrix interactions.

Piezo1 was first identified as an integrin binding protein which had a role in adhesion formation<sup>18</sup>. Our results reinforce those findings and further indicate that Piezo1 binds to a complex with the integrins but not with adhesion proteins such as talin or paxillin, which have much more rapid recovery rates after photobleaching. Further, inhibition of PTPN12 activity or expression of the *Shigella* IpaA effector stabilizes adhesion proteins even after inhibition of myosin but does not prevent Piezo1 dissociation. Piezo1's rapid dissociation upon myosin inhibition is rapidly reversed upon washout of the myosin inhibitor. The rate of

return to the adhesions is much more rapid than during initial adhesion formation, suggesting that the recruitment of Piezo1 at adhesions depends on a force sensitive protein or activation of a force-dependent enzyme that is retained at adhesion sites during myosin inhibition. In addition, after neoplastic transformation, Piezo1 no longer localizes to adhesions. Thus, it seems that rigidity-dependent maturation of Beta3 integrin adhesions and tension are required for Piezo1 localization. Further, the lack of adhesion maturation after depletion of Piezo1 supports the hypothesis that Piezo1 has an important role in the force-dependent maturation of adhesions on rigid surfaces, and this does not occur in transformed cells.

The Piezo1 dependent increase of cytoplasmic  $Ca^{2+}$  levels in transformed cells by mechanical perturbations, such as the stretching of cells, is difficult to explain in terms of fluctuations in either mechanical forces on adhesions or membrane tension. Further, few or no  $Ca^{2+}$  flickering events are observed in transformed cells whereas  $Ca^{2+}$  flickering events near adhesion sites occur in normal cells. Flickering events do not colocalize with integrins or traction forces, since the events are often closer to the cell edge than the adhesions in normal cells (Fig.5 A) and traction forces are higher in the transformed cells<sup>25</sup>. With regard to membrane tension, typical measurements of membrane tension in cells report values that are 2-3 orders of magnitude smaller than those needed to activate Piezo1 in vitro<sup>12,36</sup>. Certainly, the pattern of  $Ca^{2+}$  activation in the HFF cells in the vicinity of adhesions is consistent with previous results<sup>22,37,38</sup>, but it is not consistent with the simplistic model of very high membrane tension for the whole cell. Rather, there appear to be local activation events that involve elements from the adhesions that may alter local membrane tension/curvature or the association of membrane/cytoskeletal proteins that can modulate the mechanical gating of Piezo1 activity<sup>39-41</sup>.

An important aspect could be the mechanical activation of local proteins through cytoskeletal flow past adhesion contacts or BAR domain protein conformation changes. Since the discovery of Piezo1's role as a mechanosensitive ion channel in eukaryotic cells, the regulation mechanism of Piezo1's function in the various physiological activities of cells has been under heavy investigation<sup>8,9</sup>. The current model of Piezo1's physiological function assumes that it is diffusive in the plasma membrane and is activated locally through

membrane bilayer tension or curvature changes that occur through cytoskeletal-dependent mechanical events<sup>13,15,17,40,42</sup>. In these studies, we find that the involvement of Piezo1 in cell spreading on fibronectin is lost with cell transformation and also with spreading on collagen. In neoplastic transformed cells such as most tumor cell lines, we found that Piezo1 is diffusive and may contribute to metastatic phenotypes by elevating Ca<sup>2+</sup> signaling. Piezo1 also participates in stretch-dependent Ca<sup>2+</sup> entry and apoptosis of transformed cells<sup>26</sup>. The fact that stretch-dependent Ca<sup>2+</sup> accumulation is blocked by calpain inhibition further indicates that Piezo1 contributes to initial Ca<sup>2+</sup> release but calpain cleavage enables the higher levels of Ca<sup>2+</sup> entry that drive apoptosis<sup>26</sup>. Although Piezo1 appears in many different mechanical functions, the activation mechanism of Piezo1 is complex and both contributions from membrane tension and interaction with cytoskeletal proteins may modulate its activity<sup>39,43</sup>.

We recently showed that transformed cancer cells are depleted of rigidity sensing, local contraction units<sup>26</sup>. There is a conserved set of cytoskeletal proteins that are able to assemble into local rigidity sensing contractile structures in normal cells. After the depletion of any one of several cytoskeletal proteins critical for rigidity sensing and contractile pair assembly, the cell will be transformed and will no longer sense substrate rigidity. Transformation also involves changes in adhesion morphology and composition<sup>25</sup>. The differences in the adhesion components in normal and transformed cells that contribute to the adhesion phenotype are still an open question but the mRNA levels of over 700 proteins are altered upon transformation by tropomyosin 2.1 depletion (Unpublished observations). An important function of the rigidity sensors is in the maturation of focal adhesions that contain Piezo1 and without Piezo1 the mature adhesions do not form. This further fits with the absence of any differences between transformed cell adhesions with and without Piezo1. Thus, we suggest that both the maturation and the disassembly of focal adhesions is catalyzed by Piezo1. In addition, whether the differences in Piezo1 recruitment in the transformed and somatic cell lines are caused by changes in the molecular interactions or tension states of these cells remains an open question and await further investigation.

Our model of the function of Piezo 1 in Figure 7 emphasizes the catalytic role of  $\text{Ca}^{2+}$  entry in the life of the adhesions in normal cells. Initially the nascent adhesions seed actin filament formation and myosin bipolar filaments pull on the actin in the rigidity-sensing contractions<sup>44</sup>. If the matrix is rigid, then adhesions mature through enzymatic modifications that trigger the maturation process. Components in the adhesions are stretched by traction forces and now can bind Piezo1 which permits  $\text{Ca}^{2+}$  entry in a positive feedback cycle for the further maturation of the adhesion. However, when the concentration of Piezo1 reaches a threshold, there is increased  $\text{Ca}^{2+}$  entry and recruitment of calpain that now hydrolyzes components of the adhesion, causing the disassembly of the adhesion. The maturation process requires the rigidity sensing complex and will not occur in transformed (cancer) cells. This model indicates that covalent modification of adhesion components during maturation as well as traction force on those components are necessary for Piezo1 binding.

There is growing evidence of covalent modifications in maturing adhesions that alter adhesion as well as possibly membrane proteins in normal cells<sup>45,46</sup>. The release of  $\text{Ca}^{2+}$  near adhesions contributes to protein processing by the adhesion signaling hub, which is needed for adhesion maturation and cell growth on a rigid fibronectin matrix possibly through a calpain and DAPK dependent pathway. For example, the calpain-dependent cleavage of talin1 is needed for normal cell growth<sup>45</sup>. In transformed cells, growth appears independent of local  $\text{Ca}^{2+}$  entry at rigid matrix sites and Piezo1 is decoupled from traction forces and adhesion signaling. However, in many cancers, the elevated growth rates correlate with high levels of calpain that could amplify small  $\text{Ca}^{2+}$  leaks to support the growth activity. The rapid diffusion of Piezo1 in the transformed cells indicates that it may contact other membrane proteins and upon stretch, general changes in the plasma membrane could cause local activation of  $\text{Ca}^{2+}$  entry through membrane tension or curvature changes.

In the larger picture of adhesion maturation, there are many adhesion proteins that bind to adhesions in a force-dependent manner<sup>47,48</sup>. It is surprising, however, that the inhibition of the release of many adhesion proteins by the inhibition of PTPN12 or expression of virulence bacterial protein IpaA did not block the

release of Piezo1 upon myosin inhibition. Further, Piezo1 is strongly bound to the adhesions and has a lifetime similar to integrin  $\beta$ 3 in adhesions that depends on contractility. This indicates that a stable force sensitive component is responsible for binding Piezo1 without sensitivity to phosphatase activity. We have ruled out a role for talin1 in Piezo1 binding but there are many other proteins that could be force sensitive in the adhesions.

In addition, the integrin subtype dependence of Piezo1 localization to adhesions could be of great importance for the physiological function of Piezo1 such as vasculature development<sup>5</sup>. Piezo1 localization likely plays a critical role, in processes such as vascular development and tumor angiogenesis where both Piezo1 and  $\beta$ 3 integrins are indispensable. Piezo1 knock-out mice die as embryos due to vascular defects, and inactivation of  $\beta$ 3 inhibits the angiogenesis process. Mechanical forces such as shear forces are very important in these processes<sup>49</sup>. The force dependent co-localization of Piezo1 to  $\beta$ 3 integrin adhesions could be synergistic with downstream events and provides a mechanism of tension-dependent vascular growth that is critical in development as well as many cancer processes. Loss of Piezo1 function causes many downstream cell activities to be altered. Thus, it is important to understand how Piezo1 can be activated in the many situations where it has a role.

## *Material and methods*

### *Cell culture and constructs:*

The mEmerald-integrin  $\beta$ 3, mEmerald-integrin  $\beta$ 1, paxillin-mapple, paxillin-BFP and talin-GFP were gifts from Michael Davidson (Addgene plasmid # 56330, #54129, #54935). The piezo1-GFP-1591 and piezo1-mruby3-1591 plasmids were generated as previously described<sup>13</sup>. The RhoAV14 construct were from Schwartz lab<sup>50</sup>. TPM2.1-YFP construct is from Gunning Lab<sup>51</sup>. The A431 ipa peptide plasmid were generated as previously described<sup>52</sup>. siRNA for tropomyosin 2.1 was synthesized as previously described by Dharmacon<sup>53</sup>. siRNA for human Piezo1 was ordered from Dharmacon (ON-TARGETplus human Piezo1 siRNA, SMARTpool, L-020870-03-0010)

Human Foreskin fibroblast (HFF), HUVEC, and MCF-10A cells were obtained from ATCC. MDA-MB-231 cells were from Ruby Huang's lab. HEK293T cells with piezo1 KO were from Ardem Patpoutian's lab. CHOB2 cells stably express  $\alpha\text{V}\beta\text{3}$  and  $\alpha\text{5}\beta\text{1}$  integrins were generous gifts from Dr Siobhan A. Corbett<sup>54</sup>. Wildtype MEF<sup>55</sup> is from Jan Sap's lab. HFF, MDA-MB-231, HEK293T piezo1 KO and CHOB2 cells were cultured in 1X DMEM supplemented with 5 mM sodium pyruvate and 10% of Hi-FBS. MCF-10A cells were cultured using and HUVEC cells were cultured in endothelial growth media from Sigma.

### *Ca<sup>2+</sup> influx measurements*

The local Ca<sup>2+</sup> influx of the cells was measured following et. al. Briefly, the HFF cells were loaded with 4  $\mu\text{M}$  Ca<sup>2+</sup> indicator Cal-520-AM for 2 hours. Then the cells were detached using enzyme free dissociation media and resuspended in complete growth media. The cells were allowed to recover in suspension for 20 min before seeding on glass bottom coverslips coated with either fibronectin. After 2 hours the buffer was switched to Ringer's balanced salt and proceeded for imaging on Nikon TIRF system with pulsed laser lines to minimize photodamage of the sample<sup>56</sup>. The calcium image of each cells were acquired at 100Hz for 5000 frames. The  $\Delta\text{F}/\text{F}$  images of the cells were generated using a custom matlab script to reveal individual Ca<sup>2+</sup> influx events. Such events were tracked using the Trackmate ImageJ plugin<sup>57</sup>.

### *Cell spreading assay*

In the cell spreading assay, cells were transfected with respective plasmids 36-48 hours before experiments using Neon transfection system (Thermo Fisher) or JetOptimus chemical transfection reagent (PolyPlus) following manufacturer's recommendations. On the day of experiment, the cells were detached using an enzyme-free cell detaching buffer (Cell Dissociation Buffer, enzyme-free, PBS, Gibco), spun-down and resuspended in complete media ( 1X DMEM, 10% FBS). The suspended cells were allowed to recover by incubating in the cell culture hood for 20 min and then seeded onto glass bottom Petri dishes coated with ECM molecules of interest (10  $\mu\text{g}/\text{ml}$  collagen I, 10  $\mu\text{g}/\text{ml}$  fibronectin, 10  $\mu\text{g}/\text{ml}$  VTN-N, and 10  $\mu\text{g}/\text{ml}$  laminin for 1 hour). Imaging were done on a Nikon TIRF system with 405,488,561 and 640 laser lines.



## *Immunostaining and antibodies*

Cells of interest seeded on glass bottom Petri dishes were fixed with 4% paraformaldehyde (PFA) for 30 min at 37 degrees and was washed with 1X PBS three times. The fixed cells were permeabilized/blocked by incubation with TBST (1X TBS, 0.1% Tween-20) containing 5% Bovine Serum Albumin (BSA) overnight at 4 degrees. Primary antibodies were diluted in TBST, 5% BSA solution according to manufactures' recommendations and added to the cells overnight at 4 degrees. The stained cells were washed with 1X PBS and stained with secondary antibody for 1 hour at room temperature.

Rabbit anti-Piezo1 was from Novus Biologicals (NBP1-78446). Mouse anti-Paxillin antibody was from Merck Millipore (MAB 3060). Mouse anti-activated integrin  $\beta 1$  was from BD Biosciences (9EG7). Rat anti integrin  $\alpha v\beta 3$  was from Millipore(LM609).

## *FRAP analysis*

FRAP analyses were carried out on an ILAS2 TIRF image system similar to reported previously. Briefly, HFF or MDA-MB-231 cells transiently co-transfected with Piezo1-GFP and Paxillin-mapple, or Piezo1-mruby3 and mEmerald-integrin  $\beta 3$  were seeded on Fibronectin coated glass bottom dishes overnight. 2-5 square-shaped regions of interests (~3  $\mu$ m length) containing Piezo1 enriched adhesions were selected for each cell and bleached. The recovery of fluorescence in both fluorescent channels was observed for from 360 to 600 seconds after photobleaching. The recovery curves were normalized by dividing with average intensity of each ROI before bleaching and the average and standard deviation of the recovery were calculated.

## *Reference*

1. Pathak, M. M. *et al.* Stretch-activated ion channel Piezo1 directs lineage choice in human neural stem cells. *Proc. Natl. Acad. Sci.* **111**, 16148–16153 (2014).
2. Gudipaty, S. A. *et al.* Mechanical stretch triggers rapid epithelial cell division through Piezo1. *Nature* **543**, 118–121 (2017).

3. Li, C. *et al.* Piezo1 forms mechanosensitive ion channels in the human MCF-7 breast cancer cell line. *Sci. Rep.* **5**, 1–9 (2015).
4. Coste, B. *et al.* Piezo1 and Piezo2 Are Essential Components of Distinct Mechanically Activated Cation Channels. *Science (80-. )*. **330**, 55–60 (2010).
5. Li, J. *et al.* Piezo1 integration of vascular architecture with physiological force. *Nature* **515**, 279–282 (2014).
6. Solis, A. G. *et al.* Mechanosensation of cyclical force by PIEZO1 is essential for innate immunity. *Nature* **573**, 69–74 (2019).
7. Borbiri, I., Badheka, D. & Rohacs, T. Activation of TRPV1 channels inhibits mechanosensitive piezo channel activity by depleting membrane phosphoinositides. *Sci. Signal.* **8**, (2015).
8. Wu, J., Lewis, A. H. & Grandl, J. Touch, Tension, and Transduction – The Function and Regulation of Piezo Ion Channels. *Trends Biochem. Sci.* **42**, 57–71 (2017).
9. Murthy, S. E., Dubin, A. E. & Patapoutian, A. Piezos thrive under pressure: Mechanically activated ion channels in health and disease. *Nat. Rev. Mol. Cell Biol.* **18**, 771–783 (2017).
10. Zhao, Q. *et al.* Structure and mechanogating mechanism of the Piezo1 channel. *Nature* **554**, 487–492 (2018).
11. Poole, K., Herget, R., Lapatsina, L., Ngo, H. D. & Lewin, G. R. Tuning Piezo ion channels to detect molecular-scale movements relevant for fine touch. *Nat. Commun.* **5**, (2014).
12. Syeda, R. *et al.* Piezo1 Channels Are Inherently Mechanosensitive. *Cell Rep.* **17**, 1739–1746 (2016).
13. Cox, C. D. *et al.* Removal of the mechanoprotective influence of the cytoskeleton reveals PIEZO1 is gated by bilayer tension. *Nat. Commun.* **7**, 1–13 (2016).

14. Romero, L. O. *et al.* Dietary fatty acids fine-tune Piezo1 mechanical response. *Nat. Commun.* **10**, 1–14 (2019).
15. Ellefsen, K. L. *et al.* Myosin-II mediated traction forces evoke localized Piezo1-dependent Ca<sup>2+</sup> flickers. *Commun. Biol.* **2**, 298 (2019).
16. Zhang, T., Chi, S., Jiang, F., Zhao, Q. & Xiao, B. A protein interaction mechanism for suppressing the mechanosensitive Piezo channels. *Nat. Commun.* **8**, (2017).
17. Nourse, J. L. & Pathak, M. M. How cells channel their stress: Interplay between Piezo1 and the cytoskeleton. *Semin. Cell Dev. Biol.* **71**, 3–12 (2017).
18. McHugh, B. J. *et al.* Integrin activation by Fam38A uses a novel mechanism of R-Ras targeting to the endoplasmic reticulum. *J. Cell Sci.* **123**, 51–61 (2010).
19. Gaub, B. M. & Müller, D. J. Mechanical Stimulation of Piezo1 Receptors Depends on Extracellular Matrix Proteins and Directionality of Force. *Nano Lett.* **17**, 2064–2072 (2017).
20. Albarrán-Juárez, J. *et al.* Piezo1 and G<sub>q</sub> /G<sub>11</sub> promote endothelial inflammation depending on flow pattern and integrin activation. *J. Exp. Med.* **215**, 2655–2672 (2018).
21. Wei, C. *et al.* Calcium flickers steer cell migration. *Nature* **457**, 901–905 (2009).
22. Giannone, G. *et al.* Calcium rises locally trigger focal adhesion disassembly and enhance residency of focal adhesion kinase at focal adhesions. *J. Biol. Chem.* **279**, 28715–28723 (2004).
23. Li, F. *et al.* Dynamics and mechanisms of intracellular calcium waves elicited by tandem bubble-induced jetting flow. *Proc. Natl. Acad. Sci.* **115**, E353–E362 (2018).
24. Prevarskaya, N., Skryma, R. & Shuba, Y. Calcium in tumour metastasis: New roles for known actors. *Nat. Rev. Cancer* **11**, 609–618 (2011).

25. Yang, B. *et al.* Stopping transformed cancer cell growth by rigidity sensing. *Nat. Mater.* (2019).  
doi:10.1038/s41563-019-0507-0
26. Tijore, A. *et al.* Mechanical Stretch Kills Transformed Cancer Cells. *bioRxiv* 491746 (2018).  
doi:10.1101/491746
27. Ren, X. D. *et al.* Focal adhesion kinase suppresses Rho activity to promote focal adhesion. *J. Cell Sci.* **113**, 3673–3678 (2000).
28. Park, H., Valencia-Gallardo, C., Sharff, A., Tran Van Nhieu, G. & Izzard, T. Novel vinculin binding site of the IpaA invasin of Shigella. *J. Biol. Chem.* **286**, 23214–21 (2011).
29. Valencia-Gallardo, C. *et al.* Vinculin targeting by Shigella IpaA promotes stable cell adhesion independent of mechanotransduction. *bioRxiv* (2019). doi:10.1101/773283
30. Tullio, A. N. *et al.* Nonmuscle myosin II-B is required for normal development of the mouse heart. *Proc. Natl. Acad. Sci. U. S. A.* **94**, 12407–12412 (1997).
31. Humphries, J. D., Byron, A. & Humphries, M. J. Integrin ligands at a glance. *J. Cell Sci.* **119**, 3901–3 (2006).
32. Mas-Moruno, C., Rechenmacher, F. & Kessler, H. Cilengitide: The First Anti-Angiogenic Small Molecule Drug Candidate. Design, Synthesis and Clinical Evaluation. *Anticancer. Agents Med. Chem.* **10**, 753–768 (2011).
33. Elosegui-Artola, A. *et al.* Rigidity sensing and adaptation through regulation of integrin types. *Nat. Mater.* **13**, 631–7 (2014).
34. Taherian, A., Li, X., Liu, Y. & Haas, T. A. Differences in integrin expression and signaling within human breast cancer cells. *BMC Cancer* **11**, (2011).
35. Koistinen, P., Ahonen, M., Kähäri, V. M. & Heino, J.  $\alpha$ V integrin promotes in vitro and in vivo survival

- of cells in metastatic melanoma. *Int. J. Cancer* **112**, 61–70 (2004).
36. Dai, J. & Sheetz, M. P. Membrane tether formation from blebbing cells. *Biophys. J.* **77**, 3363–3370 (1999).
  37. Giannone, G., Rondé, P., Gaire, M., Haiech, J. & Takeda, K. Calcium oscillations trigger focal adhesion disassembly in human U87 astrocytoma cells. *J. Biol. Chem.* **277**, 26364–26371 (2002).
  38. Sen, S. & Kumar, S. Combining mechanical and optical approaches to dissect cellular mechanobiology. *J. Biomech.* **43**, 45–54 (2010).
  39. Cox, C. D., Bavi, N. & Martinac, B. Biophysical Principles of Ion-Channel-Mediated Mechanosensory Transduction. *Cell Rep.* **29**, 1–12 (2019).
  40. Lin, Y.-C. *et al.* Force-induced conformational changes in PIEZO1. *Nature* (2019). doi:10.1038/s41586-019-1499-2
  41. Shi, Z., Graber, Z. T., Baumgart, T., Stone, H. A. & Cohen, A. E. Cell Membranes Resist Flow. *Cell* **175**, 1769-1779.e13 (2018).
  42. Guo, Y. R. & MacKinnon, R. Structure-based membrane dome mechanism for piezo mechanosensitivity. *Elife* **6**, 1–19 (2017).
  43. Bavi, N., Richardson, J., Heu, C., Martinac, B. & Poole, K. PIEZO1-Mediated Currents Are Modulated by Substrate Mechanics. *ACS Nano* **13**, 13545–13559 (2019).
  44. Wolfenson, H., Yang, B. & Sheetz, M. P. Steps in Mechanotransduction Pathways that Control Cell Morphology. *Annu. Rev. Physiol.* **81**, 585–605 (2019).
  45. Saxena, M., Chagede, R., Hone, J., Wolfenson, H. & Sheetz, M. P. Force-Induced Calpain Cleavage of Talin Is Critical for Growth, Adhesion Development, and Rigidity Sensing. *Nano Lett.* **17**, 7242–7251 (2017).

46. Schwartz<sup>1</sup>, A., Hall<sup>1</sup>, C., Barney<sup>1</sup>, L., Babbitt<sup>2</sup>, C. & Peyton<sup>1</sup>, S. Mechanosensing of Integrin  $\alpha 6$  and EGFR Converges at Calpain 2. (2017). doi:10.1101/164525
47. Moore, S. W., Roca-Cusachs, P. & Sheetz, M. P. Stretchy proteins on stretchy substrates: the important elements of integrin-mediated rigidity sensing. *Dev. Cell* **19**, 194–206 (2010).
48. Galbraith, C. G., Yamada, K. M. & Sheetz, M. P. The relationship between force and focal complex development. *J. Cell Biol.* **159**, 695–705 (2002).
49. Li, J. *et al.* Piezo1 integration of vascular architecture with physiological force. *Nature* **515**, 279–282 (2014).
50. Ren, X. D., Kiosses, W. B. & Schwartz, M. A. Regulation of the small GTP-binding protein Rho by cell adhesion and the cytoskeleton. *EMBO J.* **18**, 578–585 (1999).
51. Gateva, G. *et al.* Tropomyosin Isoforms Specify Functionally Distinct Actin Filament Populations In Vitro. *Curr. Biol.* **27**, 705–713 (2017).
52. Valencia-Gallardo, C. *et al.* Cell adhesion promoted by a unique Shigella IpaA vinculin- and talin-binding site. *bioRxiv* 329136 (2018). doi:10.1101/329136
53. Wolfenson, H. *et al.* Tropomyosin controls sarcomere-like contractions for rigidity sensing and suppressing growth on soft matrices. *Nat. Cell Biol.* **18**, 33–42 (2015).
54. Ly, D. P., Zazzali, K. M. & Corbett, S. A. De novo expression of the integrin  $\alpha 5 \beta 1$  regulates  $\alpha v \beta 3$ -mediated adhesion and migration on fibrinogen. *J. Biol. Chem.* **278**, 21878–21885 (2003).
55. Su, J., Muranjan, M. & Sap, J. Receptor protein tyrosine phosphatase alpha activates Src-family kinases and controls integrin-mediated responses in fibroblasts. *Curr. Biol.* **9**, 505–11 (1999).
56. Donnert, G., Eggeling, C. & Hell, S. W. Major signal increase in fluorescence microscopy through dark-state relaxation. *Nat. Methods* **4**, 81–86 (2007).

57. Tinevez, J. Y. *et al.* TrackMate: An open and extensible platform for single-particle tracking. *Methods* **115**, 80–90 (2017).

## Figures:

Figure 1

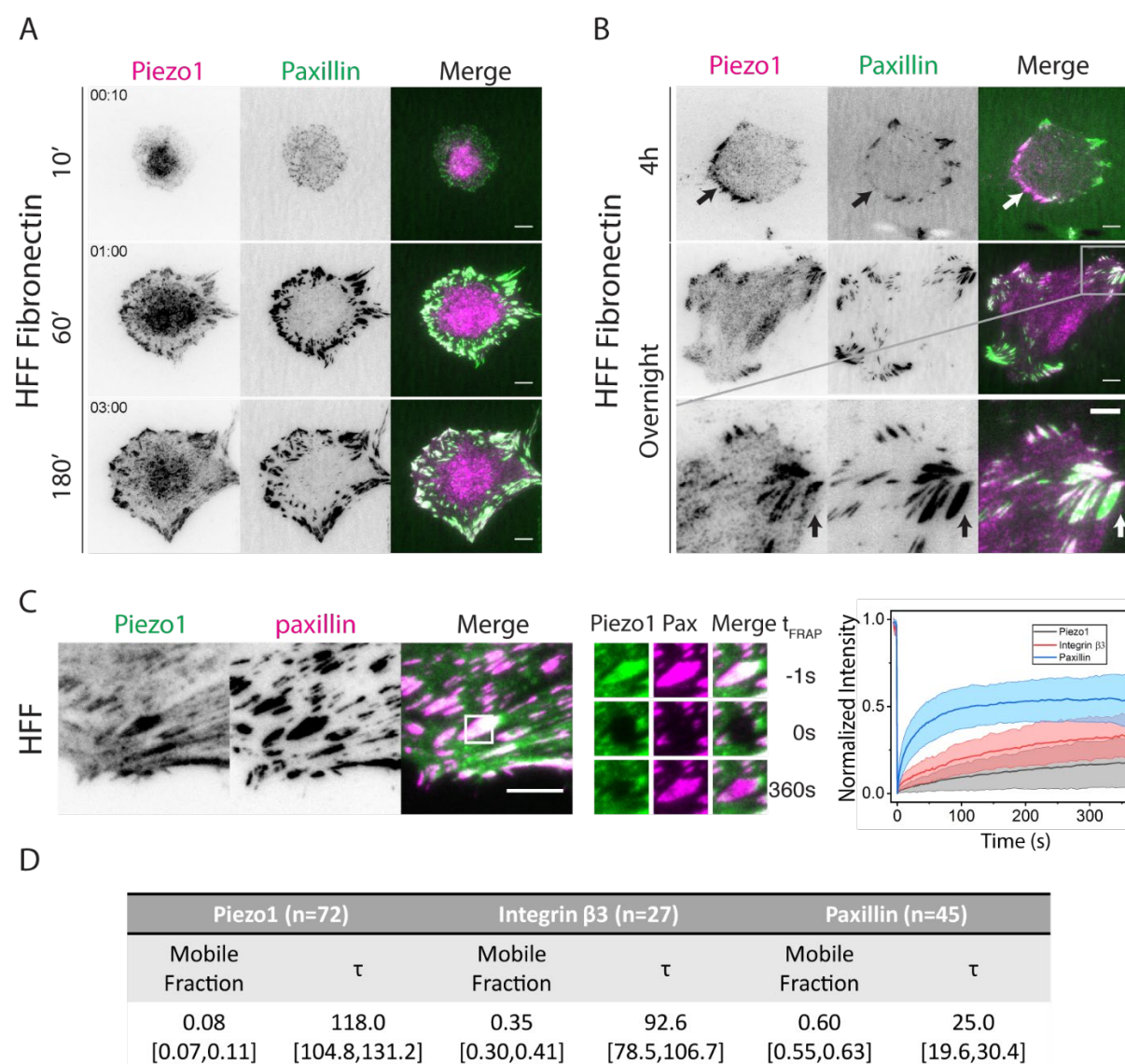
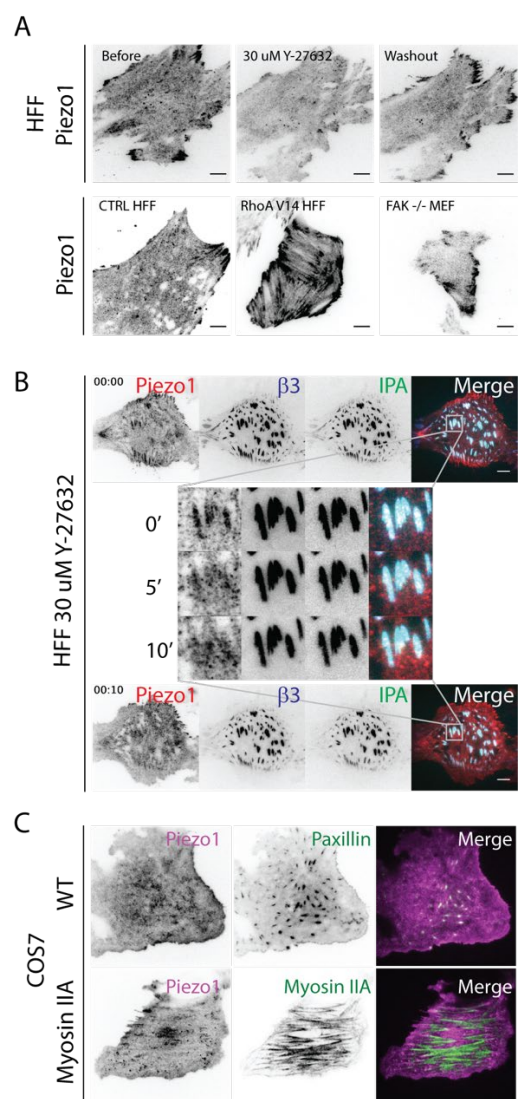


**Figure 1. Piezo1 is stably recruited to maturing adhesions on fibronectin surfaces.** **A** Time lapse of cell spreading of HFF cells seeded on fibronectin coated glass surface. The cells are transiently expressing Piezo1-mRuby3 and paxillin-BFP. **B.** Localization of Piezo1 spreading on fibronectin surface during polarization and in stable condition. **C** Left panel: Live TIRF images of Human Foreskin Fibroblast (HFF) cells transiently transfected with Piezo1-GFP and paxillin-mapple on fibronectin coated surfaces. The adhesion region marked by white square was bleached and snapshots of fluorescent recovery for Piezo1 and talin are shown in the zoom in figure on bottom. Right panel: The FRAP recovery curve of the bleached region (mean  $\pm$  std).



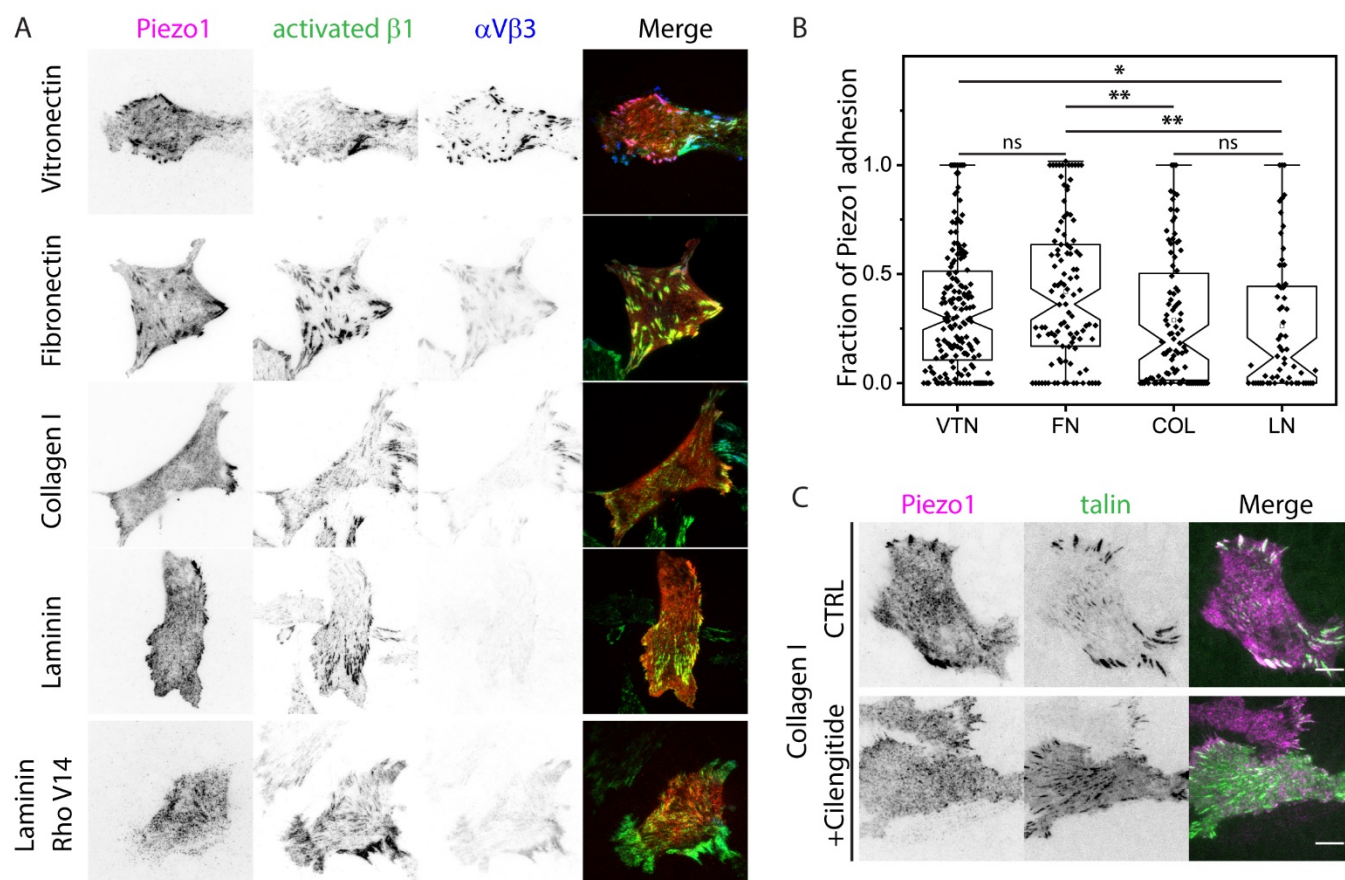
**D.** The fitted mobile fraction and recovery rates from the FRAP measurements. More than five independent cells and twenty adhesions were picked for each condition. The bracket after the fitting value denote 95% confidence interval of the fitting parameters. In the Frap experiment, Piezo1 is either co-expressed with Integrin  $\beta$ 3 or Paxillin.

Figure 2



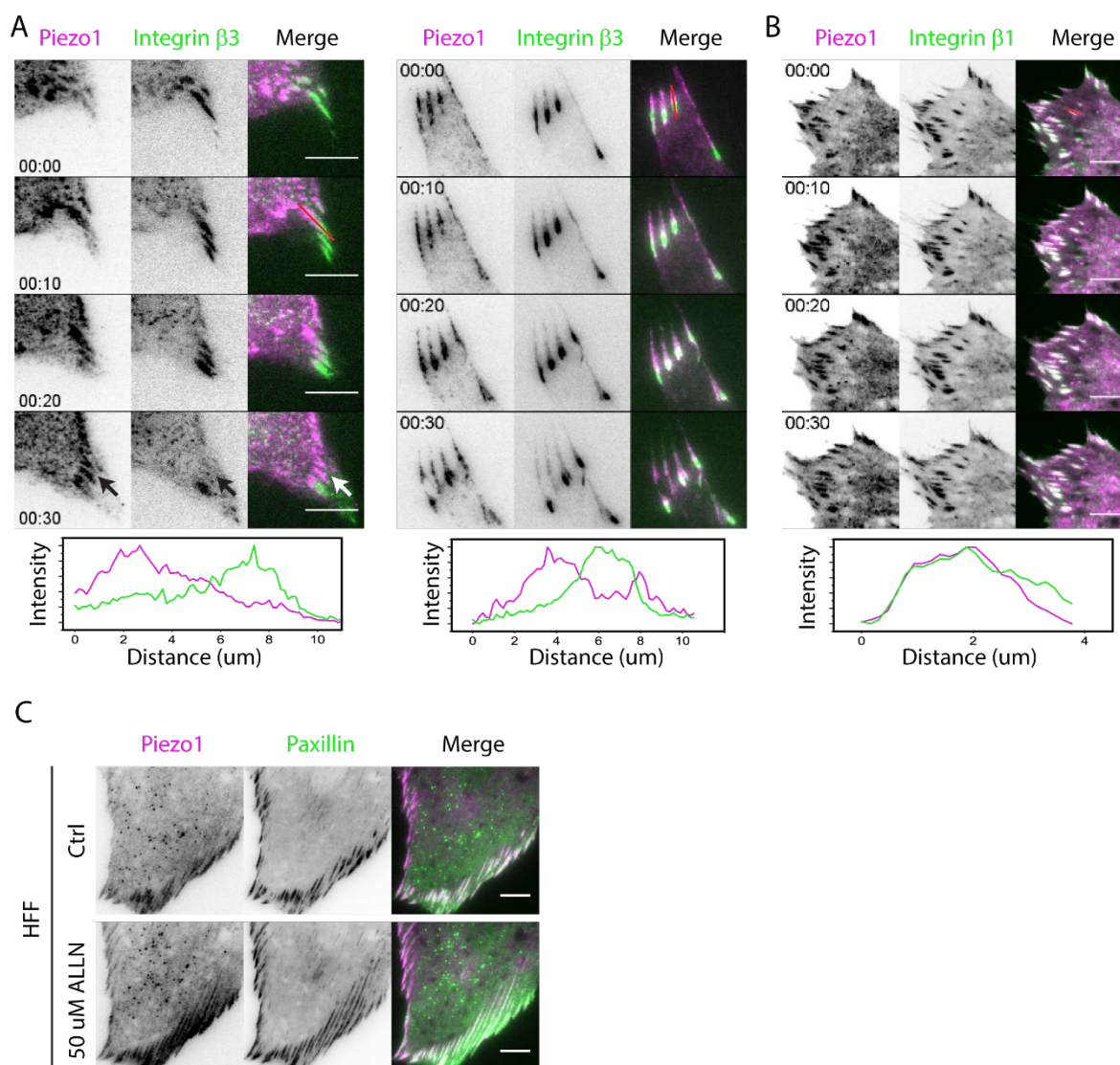
**Figure 2. Piezo1 localization in HFF cells is controlled by contractility.** **A.** Upper panel: Distribution of Piezo1-mRuby3 in HFF cells 15 min after treatment with 30  $\mu$ M Y-compound and 30 min after washout. Lower panel: representative Piezo1 localization in control HFF cells, HFF cells expressing constitutive-active RhoA and FAK-/- MEF cells where RhoA activity is elevated. **B** Time-lapse image of HFF cells transfected with Piezo1-mRuby3, integrin  $\beta 3$ -Emerald and IPA-GFP with the addition of 30  $\mu$ M Y-27632. **C** Fluorescence image of Piezo1-GFP in COS7 cells with/without overexpressing myosin IIA-mCherry.

Figure 3



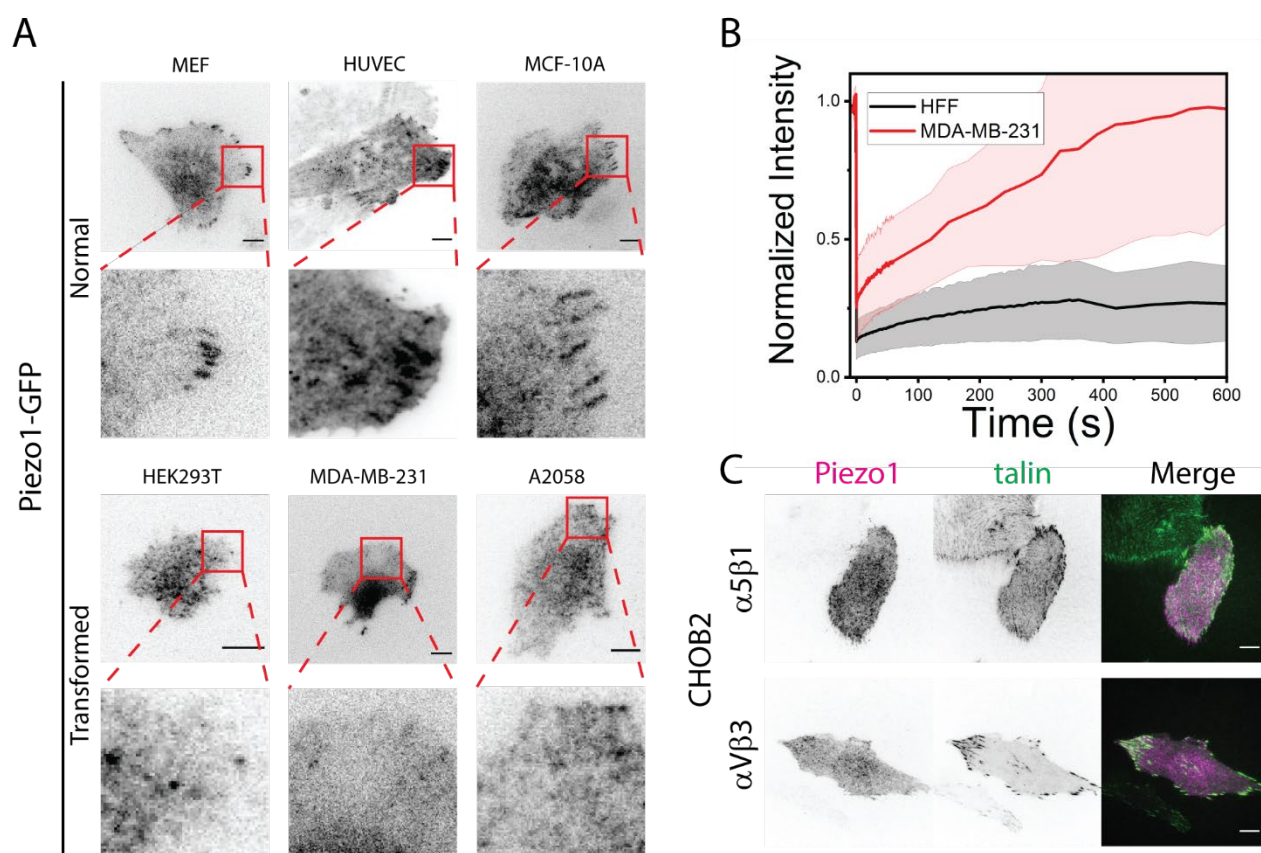
**Figure 3. Piezo1 recruitment to adhesions depend on RGD-based integrins.** (A) Fluorescence staining of representative HFF cells transfected with Piezo1-mruby3, fixed after seeding on different ECM overnight and stained for activated integrin  $\beta 1$  (9EG7 antibody) and  $\alpha V\beta 3$ . (B) Box plot of area fraction of focal adhesions with Piezo1 recruitment on different ECM substrates. More than 30 cells were measured under each condition. The significance was calculated from non-parametric Mann-Whitney test. (C) Live-imaging of HFF cells transfected with Piezo1-mruby3 and talin-GFP on collagen I surfaces overnight with or without 10  $\mu M$  RGD blocker cilengitide. Reduced Piezo1 recruitment to focal adhesions has been observed.

Figure 4



**Figure 4. Piezo1 recruitment of adhesions precede integrin  $\beta 3$  disassembly.** (A) Kymographs of HFF cells co-transfected with Piezo1-mRuby3 and mEmerald-Integrin  $\beta 3$  spreading on fibronectin surfaces. Left panel: A spreading cell one hour after seeding. Right panel: A retracting cell after overnight seeding. (B) Kymographs of HFF cells transfected with Piezo1-mRuby3 and mEmerald-Integrin  $\beta 1$  spreading on fibronectin surfaces overnight. The normalized intensity profile of adhesions highlighted by the red line were shown below the figure. (C) Elongation of Piezo1 containing adhesions upon calpain inhibition. Live imaging of HFF cells before and four hours after treatment with 50  $\mu$ M ALLN. The adhesions were marked by paxillin-mapple.

Figure 5



**Figure 5. Piezo1 localizes to the adhesions of non-transformed cells but is diffusive in transformed cells.** (A) TIRF images of Piezo1-GFP localization in various normal and transformed cell lines. (B) FRAP recovery curve of Piezo1 in HFF cells and transformed MDA-MB-231 cells. The error bar denotes standard deviation of the measurements (C) Piezo1 distribution in transformed ChoB2 cells expressing either  $\alpha 5\beta 1$  or  $\alpha V\beta 3$ .



Figure 6

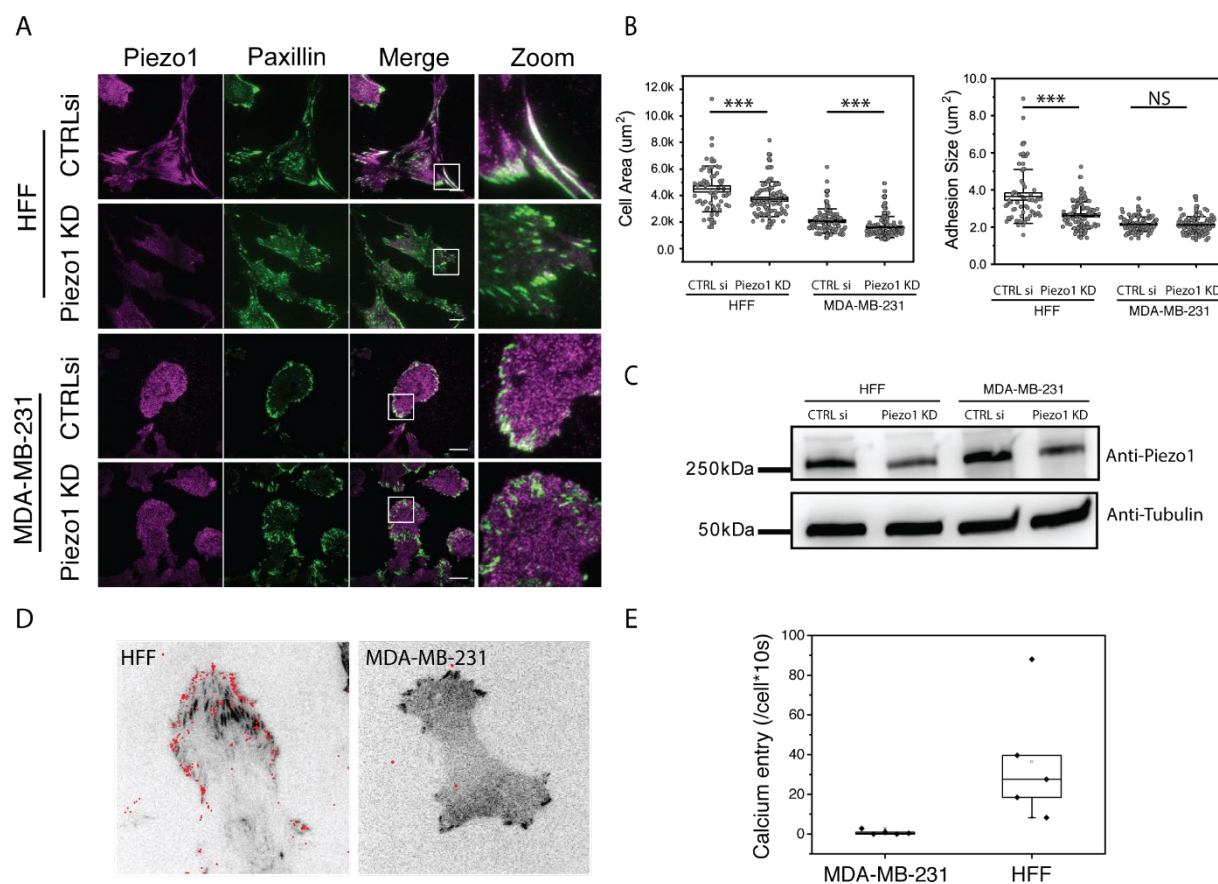


**Figure 6. Piezo1 localization affects adhesion maturation and correlates with transformation states of cells.** **A.** TIRFM image of fixed cell staining of non-transformed HFF cell line and transformed MDA-MB-231 cell line with/without Piezo1 knock down after overnight spreading on fibronectin surfaces **B.** Statistics of the cell spreading areas and mean adhesion sizes of the cells in figure A. Box and error bar denotes the s.e.m and s.t.d of the measurements. The significance value were calculated using oneway ANOVA. **C.** Western blots of Piezo1 level in control siRNA and piezo1 knock-down cells. **D.** Locations of local calcium entry events (marked by red dots) in HFF cells and MDA-MB-231 cells measured at 100 frames/s for 50s, overlaid with focal adhesions marked by paxillin. Significantly more local calcium signal is observed in HFF cells. **E.** Box plot of the rate of local calcium events per cell for HFF and MDA-MB-231 cells. Each point denotes an independent cell.

Figure 7

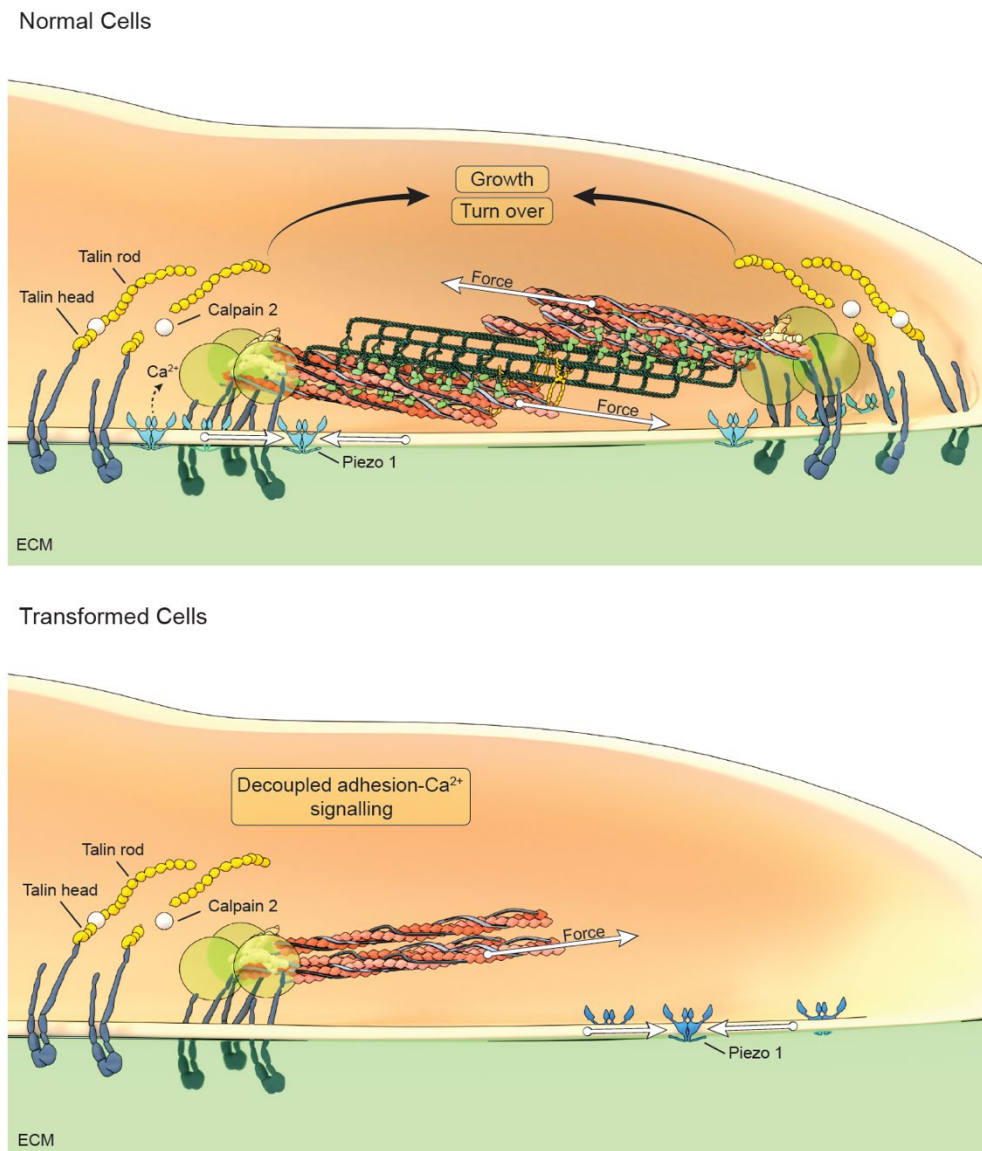
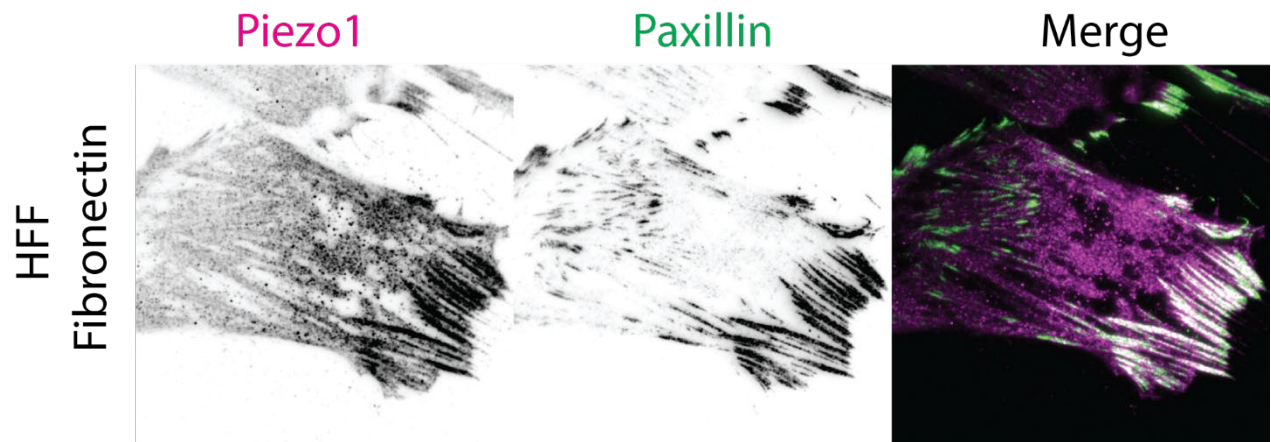


Figure 7, Model of the Piezo1's regulation in normal and transformed cells.

## Supplementary Figures

Figure S1

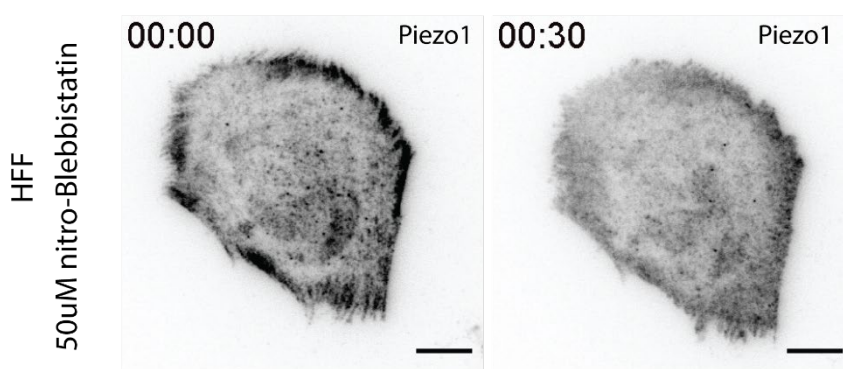


**Figure S1, Immunostaining of Piezo1 localization of HFF cells.** HFF cells were seeded on fibronectin surfaces overnight, fixed with paraformaldehyde and stained with anti-piezo1 and anti-paxillin.

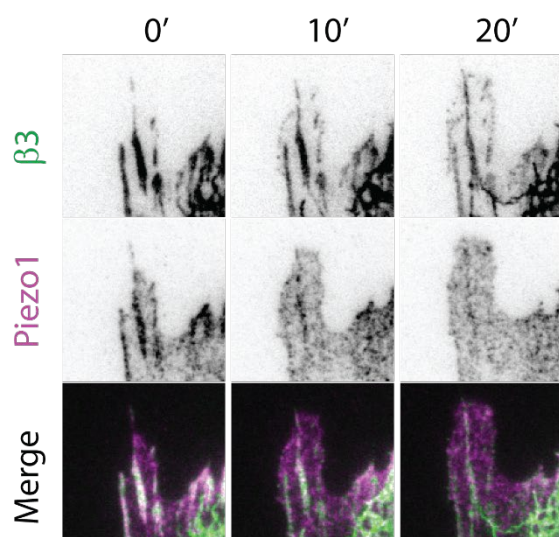


Figure S2

A

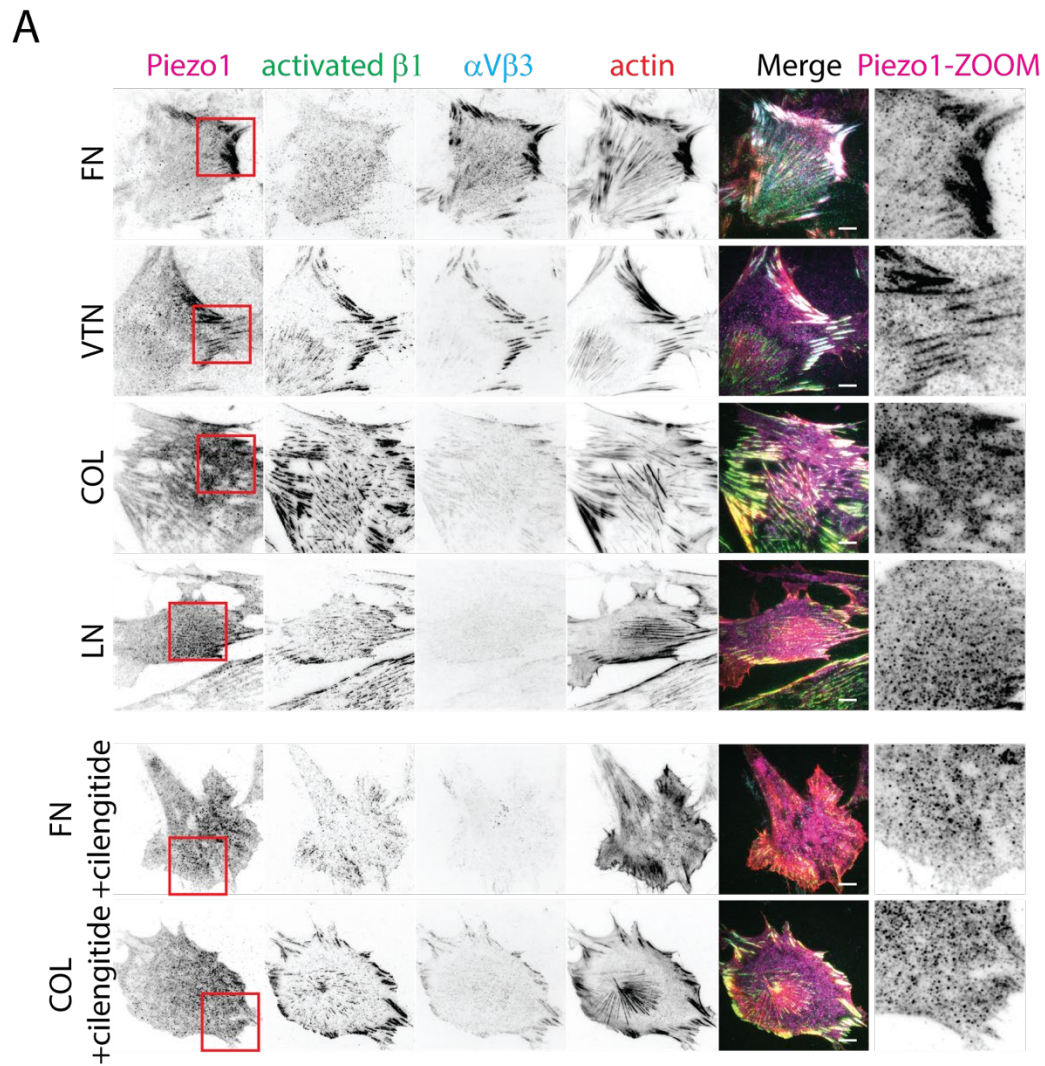


B



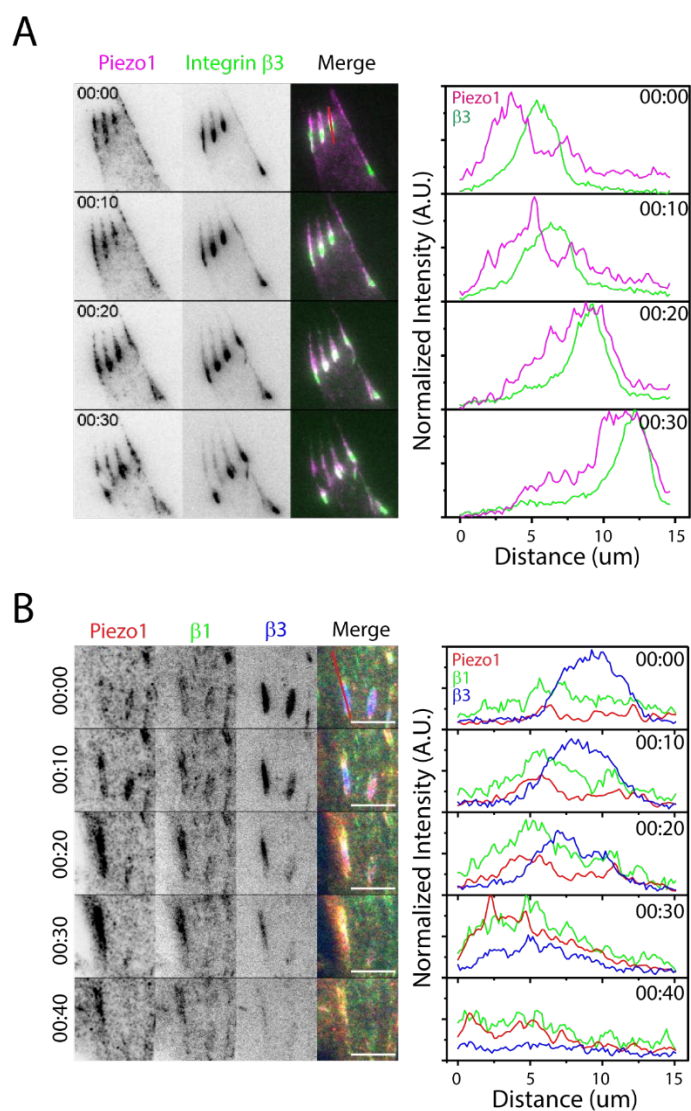
**Figure S2.** (A) HFF cells transiently transfected with Piezo1-mruby3 were treated with 50 uM nitro-Blebbistatin at time 0. After 30 min incubation, the localization of piezo1 at focal adhesions were lost. (B) HFF cells transiently transfected with mEmerald-integrin  $\beta 3$  and Piezo1-mruby3 were pre-treated with 2.5 uM PTP-PEST inhibitor that inhibits adhesion turnover by phosphatases before addition of 20 uM Y-27632. In this condition, Piezo1 dissociated from adhesions before integrin  $\beta 3$  upon tension release.

Figure S3



**Figure S3.** (A) Immunostaining of wildtype HFF cells seeded on different ECM substrates overnight. (B) Immunostaining of HFF spreading overnight on fibronectin and collagen surface overnight with the addition of the 100uM RGD-blocker cilengitide.

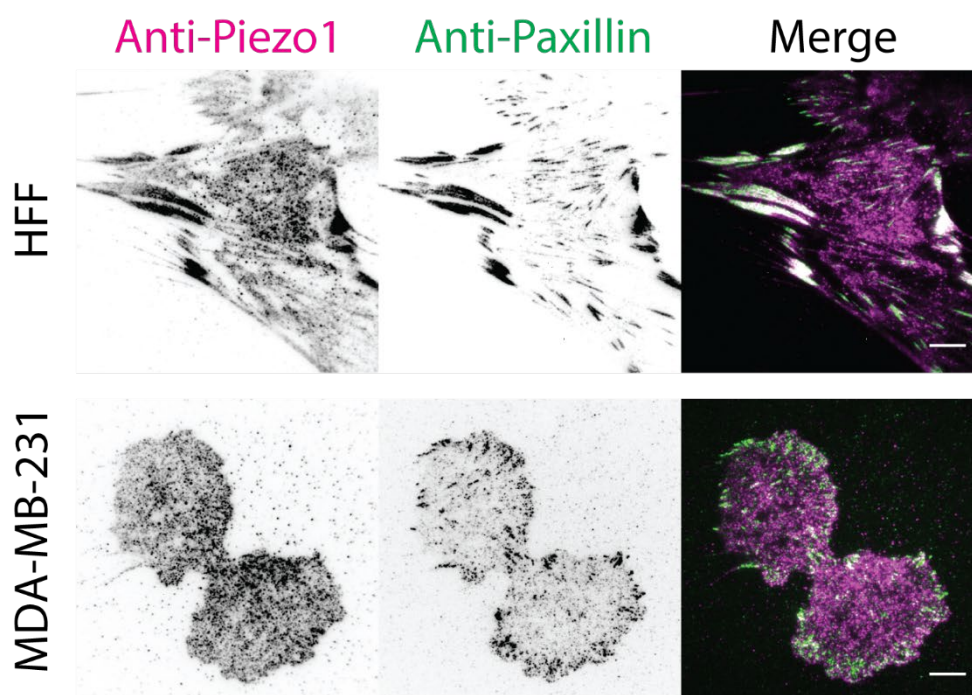
Figure S4



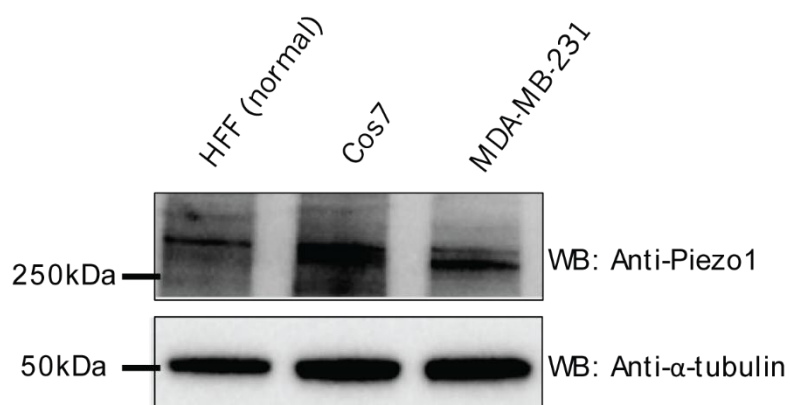
**Figure S4. Dynamics of Piezo1 localization in relation to integrins.** (A) Adhesion time lapse HFF cells transiently transfected with mEmerald-integrin  $\beta 3$  and Piezo1-mruby3. The right panel showed normalized intensity profiles of the adhesions marked by red line over time. (B) Adhesion time lapse of HFF cells transfected with BFP-integrin  $\beta 3$ , mEmerald-integrin  $\beta 1$  and Piezo1-mruby3. The right panel showed normalized intensity profiles of the adhesions marked by red line over time. The normalizations were done by dividing the intensity profiles by the maximum intensity value observed for each protein in the whole time series.

Figure S5

A



B



**Figure S5.** (A) Immunostaining of HFF cells and MDA-MB-231 cells seeded overnight on fibronectin surfaces. Clear adhesion localization of Piezo1 to focal adhesions can be observed in HFF cell but not in MDA-MB-231 cells. (B) Western blots of HFF, COS7 and MDA-MB-231 cells. For both normal and transformed cells, Piezo1 expression were detected.



Figure S6

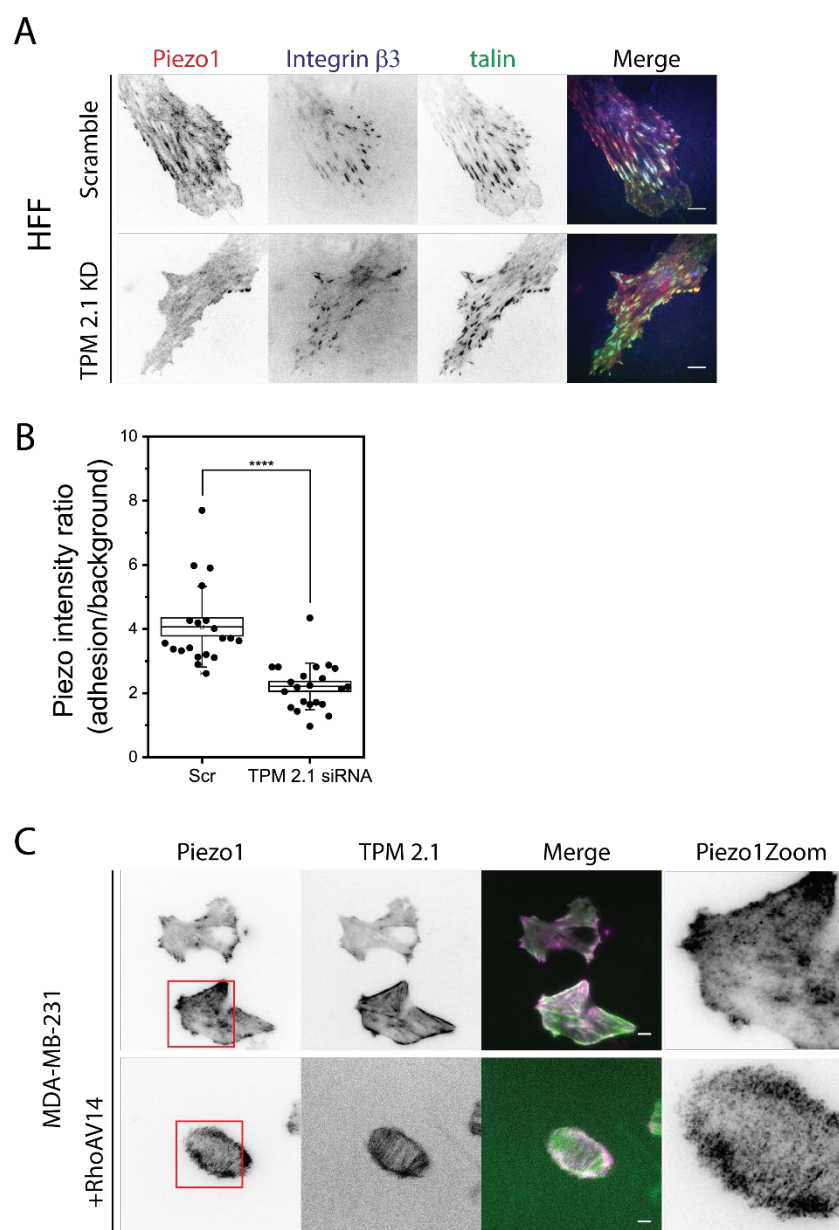


**Figure S6.** (A) Representative HFF cells with Scramble siRNA and TPM 2.1 siRNA knock down were transfected with Piezo1-mRuby3, Integrin  $\beta$ 3-BFP and talin-GFP. The cells were seeded on fibronectin surfaces overnight and imaged by TIRFM. (B) Quantification of the extent of Piezo1 recruitment to the adhesions. For each cell, three  $1 \mu\text{m}^2$  focal adhesion areas containing highest Piezo1 recruitment and three  $1 \mu\text{m}^2$  non-adhesion background areas were selected. The ratio of mean intensity between the Piezo1 enriched focal adhesion and background regions were calculated for each cell and listed in the box plot. The

box and error bars denote s.e.m and s.t.d. Significance of the differences was tested using one-way ANOVA with p-value of  $6 \times 10^{-7}$ . (C) Transient expression of TPM 2.1 -YFP in MDA-MB-231 cells led to the recruitment of Piezo1 to the end of stress fibres decorated by TPM 2.1 (TOP panel). The recruitment is enhanced by co-expression of constitutively active RhoA (Bottom panel). The images present representative cells out of > 20 imaged.